Cardiovascular Topics

Change in late sodium current of atrial myocytes in spontaneously hypertensive rats with allocryptopine treatment

Ying Dong, Yun Huang, Hong-lin Wu, Jun Ke, Yuan-li Yin, Chao Zhu, Bin Li, Jie Li, Lei Gao, Qiao Xue, Jian-cheng Zhang, Yang Li

Abstract

Aim: We aimed to study the effect of allocryptopine (All) on the late sodium current ($I_{Na,Late}$) of atrial myocytes in spontaneously hypertensive rats (SHR).

Methods: The enzyme digestion method was used to separate single atrial myocytes from SHR and Wistar–Kyoto (WKY) rats. $I_{Na,Late}$ was recorded using the patch-clamp technique, and the effect of All was evaluated on the current.

Results: Compared with WKY rat cells, an increase in the $I_{Na,Late}$ current in SHR myocytes was found. After treatment with 30 μM All, the current densities were markedly decreased; the ratio of $I_{Na,Late}/I_{Na,peak}$ of SHR was reduced by 30 μM All. All reduced $I_{Na,Late}$ by alleviating inactivation of the channel and increasing the window current of the sodium channel. Furthermore, $I_{Na,Late}$ densities of three SCN5A mutations declined substantially with 30 μM All in a concentration-dependent manner.

Conclusion: The results clearly show that an increase in $I_{Na,Late}$ in SHR atrial myocytes was inhibited by All derived from Chinese herbal medicine.

Keywords: allocryptopine, spontaneously hypertensive rats, atrial myocytes, late sodium current

Department of Cardiology, Chinese PLA General Hospital, Beijing 100853, China
Ying Dong, PhD
Hong-lin Wu, MSc
Yuan-li Yin, MSc
Chao Zhu, PhD
Bin Li, MSc
Jie Li, PhD
Lei Gao, PhD
Qiao Xue, PhD
Yang Li, PhD, liyang301pla@163.com

Department of Gerontology, Union Hospital, Tongji Medical College, Huazhong University of Science and Technology, 430022, Wuhan, China
Yun Huang, PhD

Provincial Clinical Medicine College of Fujian Medical University, Fuzhou 350001, Fujian, China
Jun Ke, PhD
Jian-cheng Zhang, PhD, 13696860345@126.com

Submitted 19/8/18, accepted 26/11/18
Cardiovasc J Afr 2019; **30**: online publication www.cvja.co.za

DOI: 10.5830/CVJA-2018-072

Atrial fibrillation (AF) is the most common arrhythmia and contributes substantially to cardiac morbidity and mortality. Many clinical studies have suggested that AF is associated with risk factors such as hypertension, aging and diabetes mellitus. Hypertension is a major risk factor for AF.[1]

The heart of the spontaneously hypertensive rat (SHR) has demonstrated inducible and even spontaneously occurring AF.[2-4] A main cause of AF is electrical remodelling with a longer action potential duration (APD) and atrial refractory period.[5] This electrical remodelling has been associated with changes in various ion currents, including an increase in the late sodium current ($I_{Na,Late}$).[6,7]

Allocryptopine (All) is an alkaloid extracted from *Corydalis decumbens* (Thunb.) Pers. Papaveraceae. Our prior studies have shown that All has potential anti-arrhythmic action in animal models, indicating that All can inhibit arrhythmias induced by aconitine with abnormal sodium currents.[8,9] Interestingly, an increase in $I_{Na,Late}$ of the SCN5A-T353I mutation, as a gene to code Nav1.5 channel protein, has been found to be greatly inhibited by All.[10] Our study focused on investigating a change in $I_{Na,Late}$ in SHR atrial myocytes and the effect of All on $I_{Na,Late}$.

Methods

Male SHR (six to eight months of age and a weight of 180–200 g) were purchased from the Experimental Animal Centre of the Chinese PLA General Hospital. Age- and gender-matched normotensive Wistar–Kyoto rats (WKY) served as controls. Research was carried out in accordance with the Guide for the Care and Use of Laboratory Animals, issued by the National Committee of Science and Technology of China.

All animals were kept in a laboratory and adapted for a week. Heart rate and blood pressure in conscious animals were measured using the tail-cuff method (CODA system, Kent Scientific, USA).

Solutions were made up as follows:

- Tyrode's solution (mM): KCl 5.4, NaCl 136, $MgCl_2$ 1.0, NaH_2PO_4 0.33, $CaCl_2$ 1.8, HEPES 10 and glucose 10 (pH 7.4).

- Kreb's buffer solution (mM): KCl 40, KOH 80, KH_2PO_4 25, $MgSO_4$ 3.0, L-glutamine 50, taurine 20, HEPES 10 glucose 10, and EGTA 0.5 (pH 7.4).
- For AP recording, the internal pipette solution contained (mM) NaCl 10, $CaCl_2$ 1, MgATP 5, KCl 120, EGTA 11, and HEPES 10 (pH 7.4). The bath solution was Tyrode's solution.
- For $I_{Na,Late}$ recording, the bath solution contained (mM) NaCl 130, $CaCl_2$ 2, $MgCl_2$ 1.2, CsCl 5, glucose 5 and HEPES 10 (7.4).
- For $I_{Na,Late}$ recording, the internal pipette solution contained (mM) cesium aspartate 80, CsCl 60, EGTA 11, HEPES 10 and Na_2ATP 5 (pH 7.2).
- Dofetilide (Dof, 5 nM) and 4-AP (5.0 mM) were added to the superfusion to block I_{Kr}, I_{KUr}, and I_{to}, respectively.

Atrial myocytes from the atrium of SHR were isolated using the double enzyme method. Briefly, each SHR was anesthetised with sodium pentobarbital (40 mg/kg), followed by anticoagulation with heparin (300 U/kg i.p.). The heart was removed immediately, suspended on a Langendorff apparatus, and then perfused via the aorta. The atrial tissue was digested with Tyrode's solution, containing type II collagenase (1.4 mg/ml, Invitrogen, USA) and trypsinase (0.24 mg/ml, Merck, Germany) for 15–20 min. Then the atrial tissue was cut into small pieces and placed in a dish containing Kreb's buffer solution. Dispersion of dissociated cardiac myocytes was facilitated by light shaking or blowing. All solutions were continuously gassed with 95% O_2 and 5% CO_2 and were maintained at 37°C.

HEK 293 cells (ATTC, Manassas, VA, USA) were maintained under 5% CO_2 in humidified air at 37°C, as indicated, for biochemical analysis. Transient transfection of SCN5A-F1473S, SCN5A-T535I and SCN5A-E1784K mutations and 2.0 µg WT cDNA plasmids pcDNA3.1 into the cultured cells was performed using lipofectamine (Life Technologies, Gaithersburg, MD, USA) as per the manufacturer's instructions. GFP cDNA was co-transfected as a reporter gene. After six hours, the transfection medium was replaced with the regular HEK293 medium. GFP-positive cells, identified using confocal imaging, were patch-clamped for recording 48 to 72 hours after transfection.

All (molecular weight 365) was obtained from the Pharmaceutical Department of Lanzhou University. It is a white crystal powder at 99.0% purity; its structure is illustrated in Fig. 1. In this study, the maximum concentration of All was selected as 0.5 mM; the drug was dissolved in dimethyl sulfoxide (DMSO) to obtain a stock solution of 1.0 M. The drug stock solution was added to the bath solution to produce the final concentration (see the Results section). At this final DMSO concentration (0.1%), no peak or sustained current was affected.

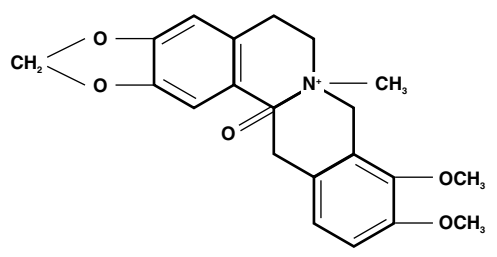

Fig. 1. Chemical formula of All, an alkaloid extracted from *Corydalis decumbens* (Thunb.) Pers. Papaveraceae.

The action potential and current were recorded with the patch-clamp technique via an Axon-700B amplifier (Axon Instruments, Inc, Foster City, CA, USA). Current signals were filtered at 3 kHz through a 16-bit A/D digital converter (Digidata 1440A; sampling rate: 1.0 kHz; Axon Instruments, Inc). Glass electrodes with tip resistances of 2.5–5.0 mΩ were used for recording. The whole-cell current was obtained under voltage clamp mode via filtering at 3.0 kHz and sampling at 10.0 kHz. The action potential was recorded in current clamp mode. Original recordings are shown in terms of current amplitude, but mean data are presented as current density for cell membrane capacitance.

Statistical analysis

Data are presented as the mean ± SD, with *n* denoting the number of cells analysed. Clampfit version 10.4 (Axon Instruments, Inc) and Origin (Microcal Software) were used for data analysis. The *t*-test was performed for two groups. Multiple groups were compared using one-way analysis of variance, and significance between any two groups was evaluated with a Student–Newman–Keuls *post hoc* test. SPSS 17.0 was used for analyses, with $p < 0.05$ considered statistically significant.

Steady-state activation (SSA) curves were fitted using a Boltzmann distribution as follows:

$$\frac{G_{(t)}}{G_{max}} = \frac{1}{1 + \exp\frac{(V_m - V_{1/2,act})}{k_{act}}}$$

where k_{act} is the slope factor and $V_{1/2,act}$ is the membrane potential for half-maximal activation.

Steady-state inactivation (SSI) was fitted using the Boltzmann equation:

$$\frac{I_{(t)}}{I_{max}} = 1 + \exp\frac{(V_m - V_{1/2,inact})}{k_{inact}}$$

where k_{inact} is the slope factor and $V_{1/2,inact}$ is the membrane potential for half-maximal inactivation.

The peak currents were measured and mean data were fitted with the Hill equation:

$$\frac{I}{I_0} = \frac{1}{1 + ([C]/IC_{50})^{nH}}$$

where [C] is the drug concentration in the external solution, IC_{50} is the half-maximum inhibited concentration, I_0 and I are the current amplitudes measured in the absence and presence of drugs, respectively, and nH is the Hill coefficient.

Results

To ensure stability of the animals, we measured their blood pressure and body weight in the first week. Results revealed

Table 1. Systolic blood pressure (SBP) and body weight of SHR and WKY rats (mean ± SD)

		Day			
Parameters	*Rats*	*1*	*3*	*5*	*7*
SBP (mmHg)	SHR	175.3 ± 10.5**	178.4 ± 14.2**	176.9 ± 7.9**	179.2 ± 13.8**
	WKY	122.4 ± 6.5	127.1 ± 7.9	120.8 ± 9.2	126.2 ± 5.4
Body weight (g)	SHR	183.5 ± 2.9	186.2 ± 4.3	184.9 ± 2.1	185.6 ± 3.1
	WKY	189.4 ± 3.4	190.2 ± 2.0	187.3 ± 4.0	188.5 ± 3.4

** $p < 0.01$ vs WKY group.

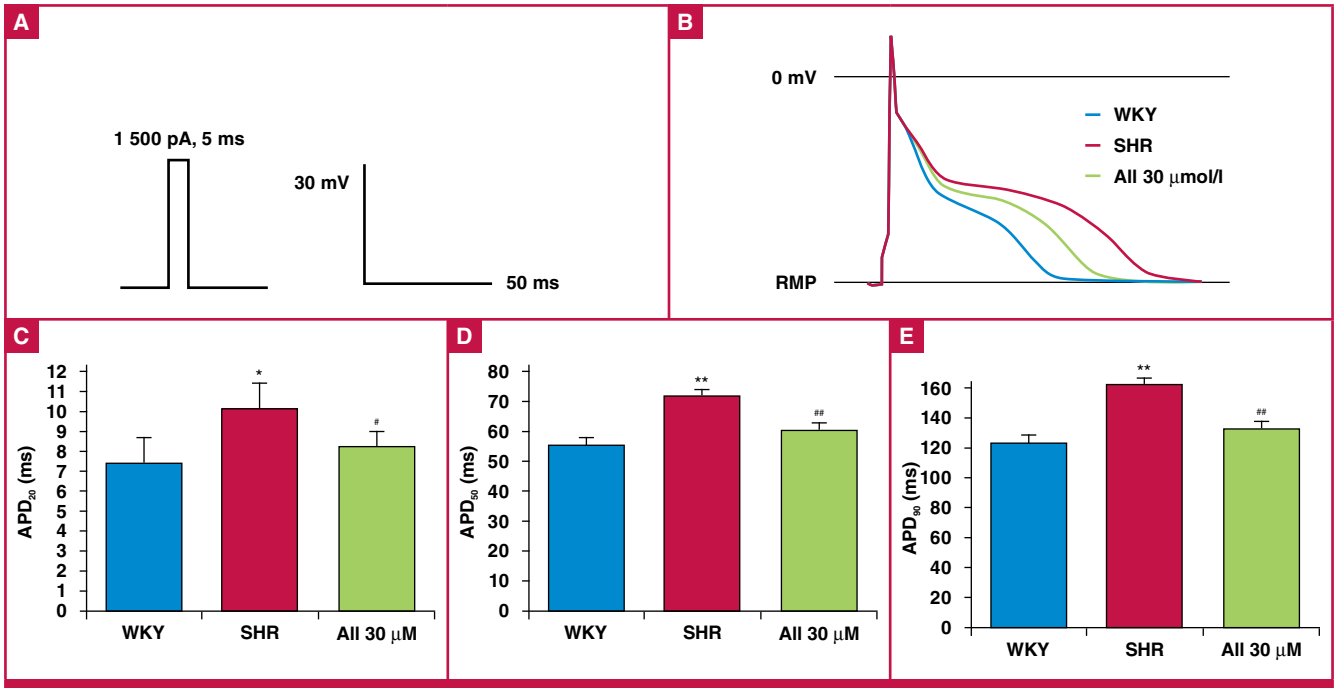

Fig. 2. Effects of All on AP. (A) Representative AP traces recorded from WKY and SHR cells with 30 μM All. $I_{Na,Late}$ of SHR myocytes. (B–D) APD_{20}, APD_{50}, and APD_{90} of atrial myocytes in SHR were markedly prolonged compared to those of WKY cells, which were significantly shortened after exposure to 30 μM All. *$p < 0.05$, **$p < 0.01$ vs WKY group. #$p < 0.05$, ##$p < 0.01$ vs SHR group.

significant differences in blood pressure between the SHR and WKY groups ($p < 0.01$, $n = 15$), whereas the weight of the two groups neither changed nor differed significantly (Table 1).

Action potential (AP) was elicited using 1 500 pA and a 5-ms current pulse. Action potential durations (APD_{20}, APD_{50} and APD_{90}) were recorded at 20, 50 and 90% repolarisation. APD_{50} and APD_{90} were prolonged in SHR atrial myocytes ($p < 0.05$ or $p < 0.01$, $n = 15$). These changes could be partially recovered by All 30 μM ($p < 0.05$ or $p < 0.01$, $n = 15$). APD_{20} changed slightly in the three groups. The resting membrane potential and the AP amplitudes showed no significant difference with 30 μM All treatment (Fig. 2).

Change of late sodium current before and after All treatment

For $I_{Na,Late}$ at steady state, we used a 500-ms depolarisation pulse before and after treatment with 30 μM All. At a test potential of –20 mV, the $I_{Na,Late}$ densities were increased from 0.24 ± 0.02 pA/pF for the WKY cells to 1.73 ± 0.04 pA/pF for the SHR cells ($p < 0.01$, $n = 15$; Fig. 3A).

After treatment with 30 μM All, current densities of SHR cells decreased to 0.92 ± 0.03 pA/pF. The ratios of $I_{Na,Late}/I_{Na,peak}$ for the WKY and SHR cells were 0.09 ± 0.01% and 0.71 ± 0.02%, respectively. The $I_{Na,Late}/I_{Na,peak}$ of the SHR group reduced to 0.37 ± 0.02% with 30 μM All ($p < 0.01$, $n = 15$; Fig. 3B).

The $I_{Na,peak}$ was elicited using depolarising steps to –40 mV for 500 ms, from a holding potential of –120 mV. Current amplitudes were normalised to the cellular membrane capacitance in the form of current densities. Compared with WKY cells, the peak current densities of SHR cells changed slightly from –248.22 ± 25.34 pA/pF to –242.82 ± 20.08 pA/pF, and the peak current density of SHR cells was –245.25 ± 17.33 pA/pF in the presence of 30 μM All (Fig. 3C).

Concentration-dependent tests of All on $I_{Na,Late}$ (1, 3, 10, 30, 100, 300, and 500 μM) were performed. $I_{Na,Late}$ was inhibited by All in a concentration-dependent manner. Plots of the IC_{50} obtained for the drug are presented in Fig. 3D. The IC_{50} of All was 16.8 ± 2.2 μM, and the Hill coefficient was 0.96.

SSA was studied by applying depolarising pulses, ranging from –100 mV to +40 mV, for 500 ms. Conductance of various voltage pulses were normalised to the maximum conductance recorded to obtain the activation curve, which was fitted to a standard Boltzmann distribution function. The $V_{1/2,act}$ of the SHR cells showed a slight negative shift compared with WKY cells. $V_{1/2}$ and k were not significantly changed with exposure to 30 μM All.

SSI was studied by applying 1 000-ms pre-pulses ranging from –140 to 0 mV, followed by a 100-ms test pulse at –20 mV. The normalised currents were fitted to a Boltzmann distribution function. During SSI, a +17.2-mV shift for the SHR cells was observed compared to the WKY cells. The SSI curve shifted positively, and then the larger window current appeared. With 30 μM All, the SSI curve shifted negatively, and the window currents in the SHR cells reduced, as shown in Fig. 4 ($p < 0.05$, $n = 15$).

The effect of All on the fast inactivation kinetics of I_{Na} was analysed. Depolarising steps from 2 to 50 ms were tested to ensure full current decay. Compared with the WKY cell channel, a significantly longer time constant of the slow component (Tau 2, indicating a decelerated inactivation of the open channel) of the SHR cells was found over a range from –70 mV to +20 mV. The fast time constant (Tau 1) proportion of the SHR cells did not change. Further, Tau 2 from the SHR cells appeared shorter after exposure to 30 μM All, but Tau 1 was not different from that of the WKY control (Fig. 5A).

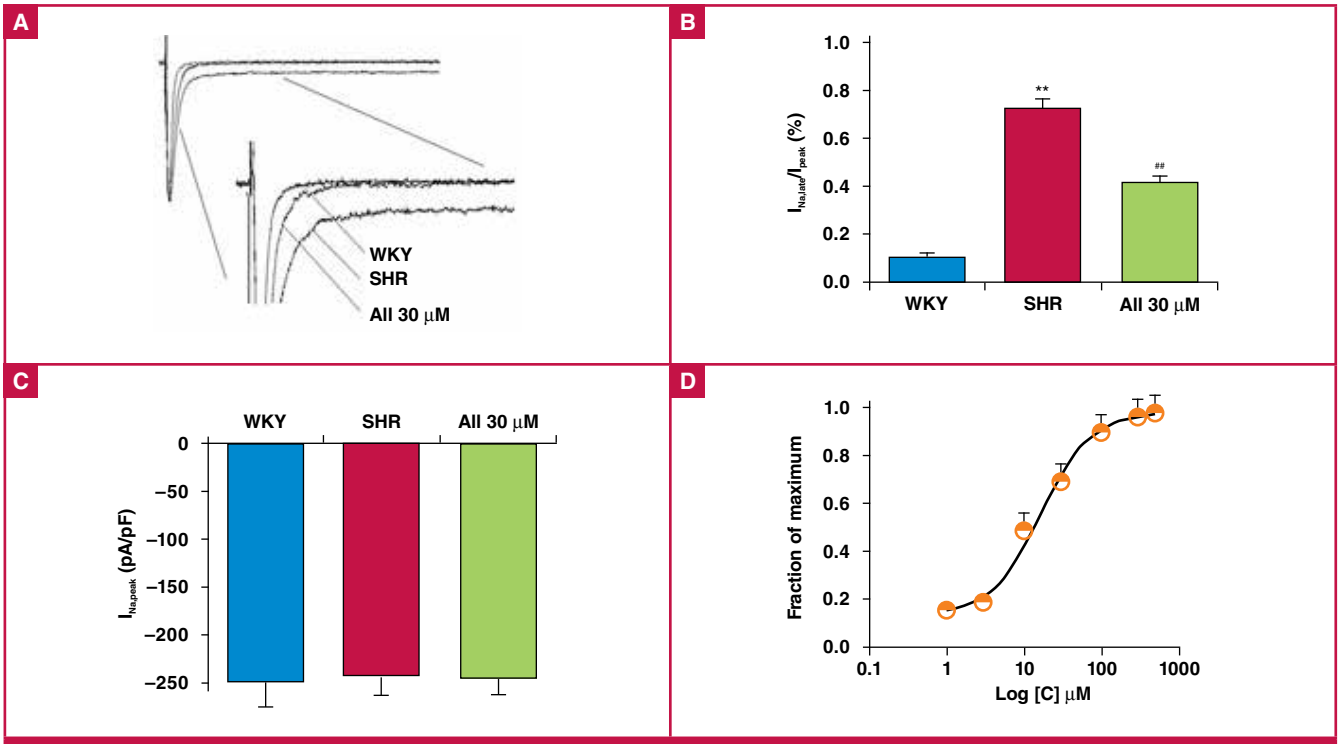

Fig. 3. Effect of All on late sodium current ($I_{Na,Late}$) of SHR myocytes. (A) Representative current traces recorded from WKY and SHR cells with 30 μM All. $I_{Na,Late}$ of SHR myocytes was significantly larger than that of WKY cells, which was inhibited by All. (B) Incremental ratio of $I_{Na,Late}/I_{Na,peak}$ in SHR cells reduced from 0.71 ± 0.02 to 0.37 ± 0.02% and ended at 0.09 ± 0.01% of WKY cells. (C) At a test potential of –20 mV, $I_{Na,peak}$ did not change in the three groups. (D) $I_{Na,Late}$ was inhibited by All in a concentration-dependent manner. IC_{50} was 16.8 ± 2.2 μM, Hill coefficient: 0.96 (n = 15). $^{**}p < 0.01$ vs WKY group. $^{\#\#}p < 0.01$ vs SHR group.

With the double-pulse protocol, recovery from the current inactivation process was measured. Cell currents were pre-pulsed to –20 mV for 100 ms, according to the interval times (0.5, 1, 2, 5, 10, 20, 50, 100, 200 and 500 ms) at –120 mV, and then stepped up to –20 mV. The recovery constants of the three groups were not markedly different (n = 15; Fig. 5B).

To determine the exact action of All on the late sodium current, we investigated whether All exerted a direct effect on three SCNA5A mutations (F1473S-SCN5A, T535I-SCN5A and E1784K-SCN5A) with a late sodium current in HEK293 cells. The current was induced using 500-ms depolarisations before and after treatment with 30 μM All. Representative current traces of F1473S-SCN5A, T535I-SCN5A, E1784K-SCN5A and WT of SCN5A are shown in Fig. 6A. At a test potential of –20 mV, the $I_{Na,Late}$ densities of the three mutations increased from 0.81 ± 0.03 pA/pF for the WT to 5.02 ± 0.13 pA/pF for F1473S, 594 ± 0.47 pA/pF for T535I, and 4.12 ± 0.12 pA/pF for E1784K, respectively ($p < 0.01$, n = 10). After exposure to 30 μM All, the $I_{Na,Late}$ densities of SCN5A mutations decreased to 1.08 ± 0.02 pA/pF for F1473S, 1.32 ± 0.50 pA/pF for T535I, and 0.97 ± 0.31 pA/pF for E1784K, respectively ($p < 0.01$, n = 10; Fig. 6B).

The effects of different concentrations of All on $I_{Na,Late}$ of the SCN5A mutations were investigated. $I_{Na,Late}$ was inhibited by All in a concentration-dependent manner. IC_{50} was 15.2 ± 2.2 μM for F1473S, 41.8 ± 3.6 μM for T535I, and 18.1 ± 3.2 μM for E1784K, respectively. The Hill coefficients were 0.87, 1.29 and 0.98, respectively (Fig. 6C).

Discussion

In epidemiological studies, the risk of AF was estimated to be 1.42 times higher in hypertensive patients compared with normotensives. Hypertension, age and diabetes are prominent risk factors for AF.[11,12] Normally, the sodium channel was inactivated within a few milliseconds of depolarisation. Some channels remained open, creating a small but persistent influx of Na^+ throughout the plateau of AP during pathological conditions.[13,14]

Especially in chronic physiological and pathological processes (such as in the case of aging, myocardial hypertrophy, sick sinus syndrome and heart failure), sodium channels may be remodelling. Chang *et al.* found down-regulation of Nav1.5 protein expression and reduced I_{Na} density in failing hearts and ischaemia–reperfusion injury. Nav1.5 contributes to arrhythmogenesis in heart failure due to the generation of $I_{Na,Late}$.[15] Up-regulated Nav1.8 augmented $I_{Na,Late}$ in human hypertrophied myocardium and prolonged the APD.[16,17]

Sick sinus syndrome is a common arrhythmia often associated with aging or organic heart diseases. The disease-causing gene is closely related to the sodium channel.[18] The SHR cells showed electrophysiological remodelling of the left atrium, leading to increased vulnerability to burst pacing-induced atrial arrhythmias.[2]

Our investigation demonstrated larger $I_{Na,Late}$ and longer APD in SHR atrial cells compared with WKY cells. The magnitude of $I_{Na,Late}$ may increase significantly in chronic pathological settings. Sossalla *et al.*[19] reported that $I_{Na,Late}$ increased in atrial

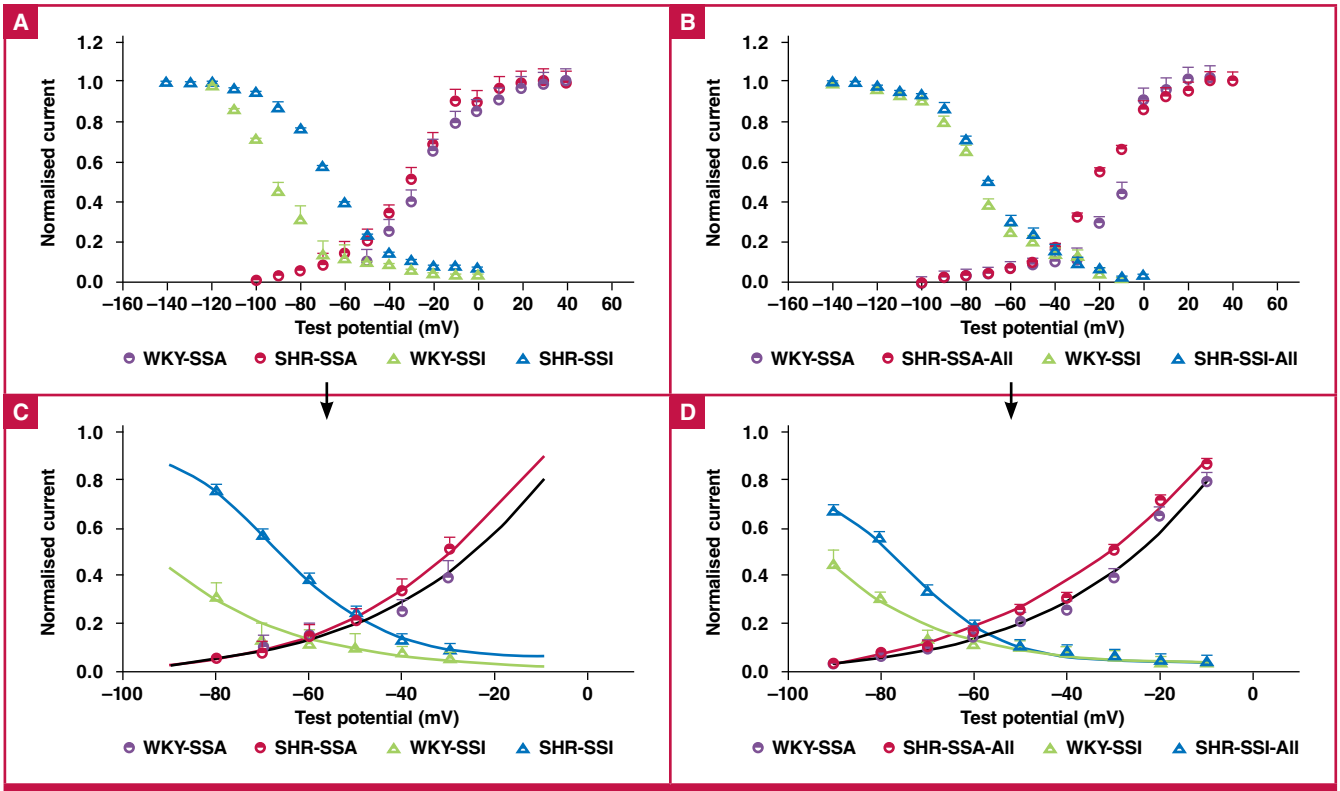

Fig. 4. Effects of All on steady-state activation (SSA) and steady-state inactivation (SSI) of I_{Na}. (A) SSA and SSI curves are shown. SSI curves differed between WKY and SHR. (B) In the presence of 30 μM All, SSI curves were shifted to positive potentials (n = 15). Amplified images of the local graphics from (A) and (B) are shown in (C and D). (C) Larger windows of current of SHR cells (red crossing line) than that of WKY cells (black crossing line). (D) Windows of current of SHR cells reduced by 30 μM All (red crossing line) and close to that of WKY (black crossing line).

myocytes isolated from the right atrial appendage of persistent AF patients. $I_{Na,Late}$ densities in left atria have also been reported to increase in a rabbit left ventricular hypertrophy model caused by hypertension.[13]

$I_{Na,Late}$ contributes to the plateau phase of the cardiac AP and is related to arrhythmogenesis under pathological conditions. Although the contribution is small relative to the peak current, $I_{Na,Late}$ cannot be neglected. A small, persistent Na^+ current prolongs the plateau APD and induces a Na^+ load that may indirectly increase intracellular Ca^{2+} concentrations. Both AP prolongation and Ca^{2+} overload are reported to be the main causes of AF.[20,21] Our findings suggest that enhanced $I_{Na,Late}$ is involved in the occurrence and development of AF.

We also found that the window currents of SHR atrial cells were enhanced. Several factors contribute to the late sodium current, in which an increase in the window current is a driving

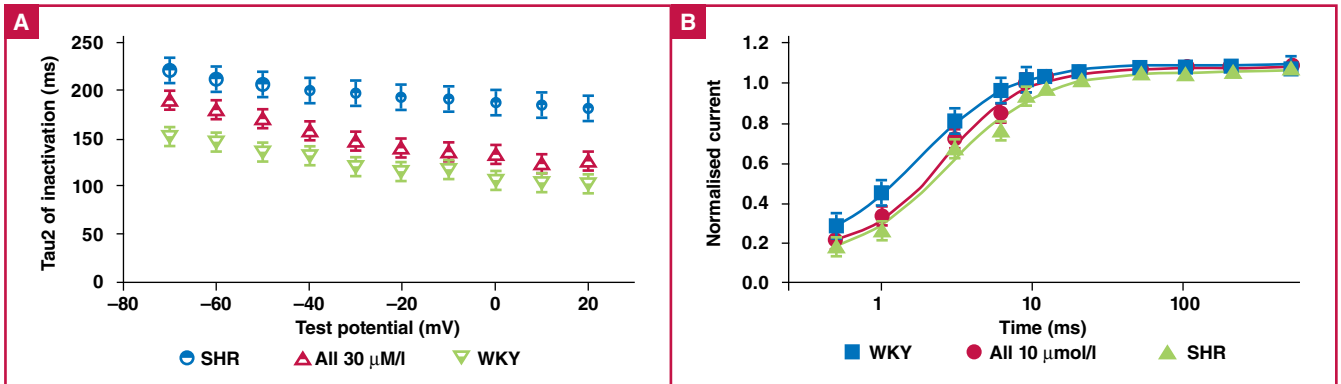

Fig. 5. Effect of All on inactivation of kinetic characteristics and recovery from inactivation of currents of SHR. Channel from SHR cells demonstrated a significantly longer time constant of the slow component (Tau 2) compared with the WKY cell channel over the entire voltage range from –70 mV to +20 mV. (A) Tau 2 from SHR cells appeared shorter after exposure to 30 μM All (n = 15). (B) Recovery curve from inactivation was slightly different in SHR, WKY and All group cells but not statistically significantly different.

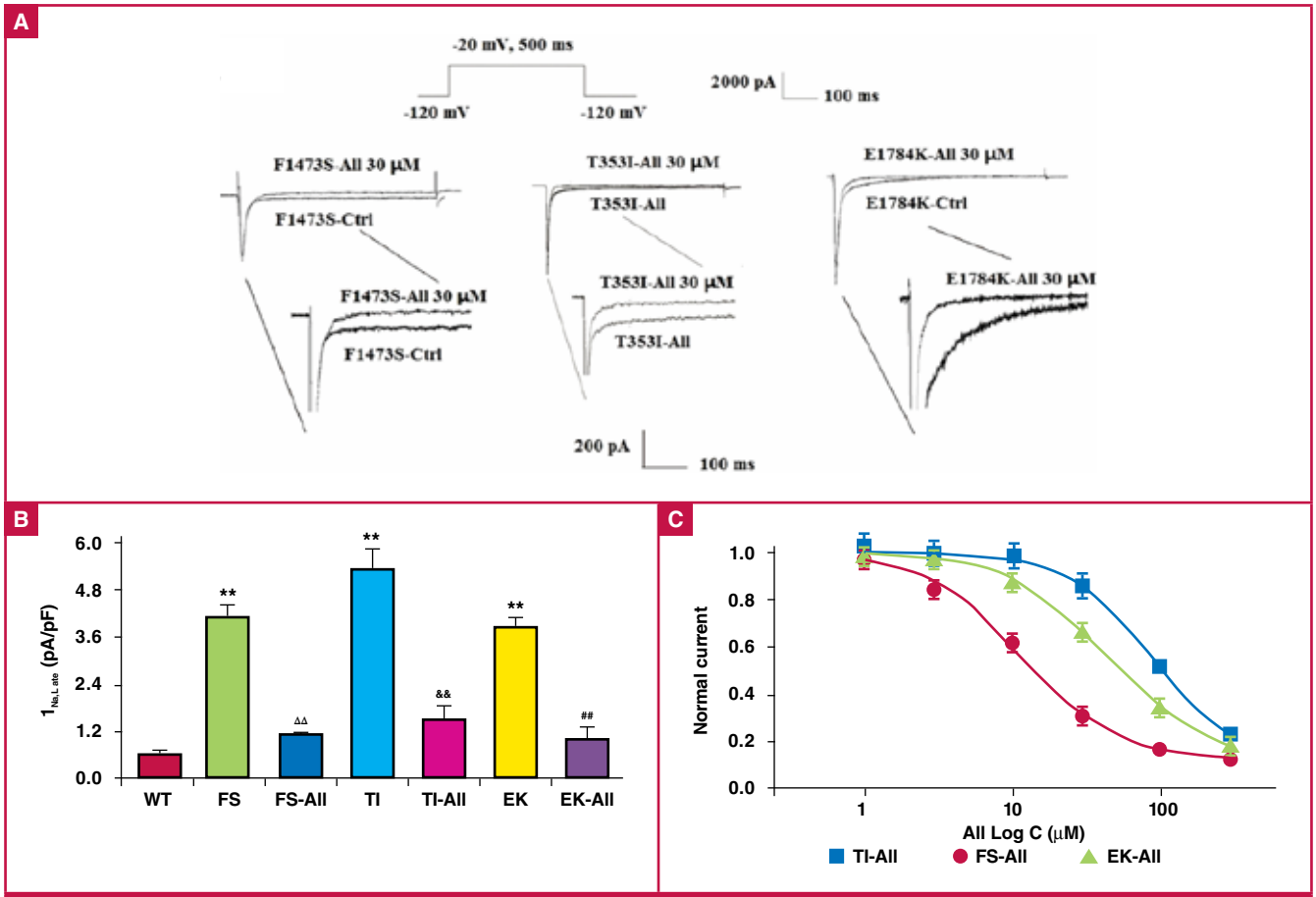

Fig. 6. Effect of All on $I_{Na,late}$ of three SCN5A mutations in HEK293 cells. (A) Representative $I_{Na,late}$ current traces recorded from WT, F1473S, T353I and E1784K before and after exposure to 30 μM All. (B) At a test potential of –20 mV, $I_{Na,late}$ current densities of F1473S, T353I and E1784K increased significantly compared with WT. After exposure to 30 μM All, $I_{Na,late}$ current densities decreased significantly. (C) Inhibition effects of All on $I_{Na,late}$ in a concentration-dependent manner. IC_{50} was 15.2 ± 2.2 μM for F1473S, 41.8 ± 3.6 μM for T535I, and 18.1 ± 3.2 μM for E1784K. $^{**}p < 0.01$, compared with WT. $^{\Delta\Delta}p$, $^{\&\&}p$ and $^{\#\#}p < 0.01$, compared with FS, TI and EK, respectively.

mechanism, namely in the overlap of the SSA and SSI of the sodium channel.[22] The window current is increased by the late sodium current, thereby extending the APD. The mutations in SCN5A delay repolarisation, relating to long QT syndrome 3 (LQT3), mostly by increasing $I_{Na,Late}$ and increasing the window current, owing to the right shift in the inactivation curve to slow the inactivation course of the sodium channel.[23]

Our study demonstrated that All greatly reduced the $I_{Na,Late}$ of SHR atrial cells. All caused voltage- and concentration-dependent $I_{Na,Late}$ inhibition with an IC_{50} of 16.8 ± 2.2 μmol/l and a Hill coefficient of 0.96. All appeared to bind at the binding site of the cardiac-specific Na channel isoform Nav1.5 with SCN5A coding. Another LQT3 mutation, F1473S, was reported by Ran *et al.*,[24] showing that an enlarged window current induced an $I_{Na,Late}$ that was not affected by mexiletine (a sodium channel inhibitor).

$I_{Na,Late}$ may be a cause of after-depolarisations, spontaneous diastolic depolarisation, and triggered arrhythmias in atrial myocytes. In addition, $I_{Na,Late}$ increases repolarisation dispersion and may lead to APD alternans and re-entrant arrhythmias. Several kinds of $I_{Na,Late}$ inhibitors have shown promising clinical effects.[25,26] Ranolazine, a $I_{Na,Late}$ blocker, demonstrated anti-AF effectiveness in persistent AF patients.[27] Other drugs may preferentially inhibit $I_{Na,Late}$, including anti-arrhythmic drugs in class I (mexiletine, lidocaine and flecainide) and class III (amiodarone).[28]

Our findings reveal selective inhibition of All on $I_{Na,Late}$ of atrial myocytes from SHR in a concentration-dependent manner. In previous studies, we found that All could reduce delayed after-depolarisations and trigger activities in mice cardiomyocytes induced by isoproterenol.[9,29] This discovery provides evidence for the inhibition of atrial ectopic rhythm and a reduction in AF.

All may rescue trafficking deficiencies and restore the cellular electrophysiological characteristics of SCN5A-T353I, causing Brugada syndrome and LQT3.[10] We also found that All decreased transmural repolarising ionic ingredients of outward potassium current (I_{to}) and slowly delayed the rectifier potassium current (I_{Ks}).[8] These findings provide a novel perspective on the application of All in atrial anti-arrhythmogenesis in clinical settings.

Limitations

Electrical remodelling of atrial myocytes is found in age and chronic disease conditions. More recently, Yan *et al.*[30] reported that the stress-response kinase JNK isoform 2 (JNK2) plays

an important role in promoting atrial arrhythmias. JNK is activated in response to various cellular stresses such as aging, ischaemia, inflammation, cardiac hypertrophy and alcohol use.[31-33] Their results showed that JNK2 activation caused abnormal intracellular calcium waves and diastolic sarcoplasmic reticulum Ca^{2+} leak in the atrial myocytes.[30] $I_{Na,Late}$ is enhanced in the myocytes of animals with chronic heart failure and patients with hypertrophic cardiomyopathy. We do not know how the JNK changed in the SHR atrial myocytes, and whether it affected the late sodium current. The effect of AII on the JNK signalling pathway requires further research.

$I_{Na,Late}$ may increase calcium influx via the reverse mode of the sodium/calcium exchanger. Intracellular Ca^{2+} levels increase and cause a series of pathophysiological changes, such as structural and electrical remodelling of the atrium. In this study, we focused on the effect of AII on the $I_{Na,Late}$ from SHR atrial myocytes. The change in Ca^{2+} concentration and its molecular regulation of signalling pathways was not explored. It would be necessary to investigate the concentration of Ca^{2+} and the activity of CaMKII in SHR atrial cells.

Conclusion

This study is the first to demonstrate the direct inhibitory effect of AII on the $I_{Na,Late}$ current in SHR atrial myocytes in a concentration-dependent fashion. The underlying mechanisms may be partially explained by their roles in reducing the sodium channel window current. This provides, at least in part, a potential for the application of AII in anti-arrhythmia patients.

We thank the members of our laboratories for their insight and technical support, and also the National Natural Science Foundation of China (grant no. 81870249, 81671731, 81470542).

References

1. Schotten U, Verheule S, Kirchhof P, Goette A. Pathophysiological mechanisms of atrial fibrillation: a translational appraisal. *Physiol Rev* 2011; **91**: 265–325.
2. Choisy SC, Arberry LA, Hancox JC, James AF. Increased susceptibility to atrial tachyarrhythmia in spontaneously hypertensive rat hearts. *Hypertension* 2007; **49**: 498–505.
3. Scridon A, Gallet C, Arisha MM, Oréa V, Chapuis B, Li N, *et al*. Unprovoked atrial tachyarrhythmias in aging spontaneously hypertensive rats: the role of the autonomic nervous system. *Am J Physiol Heart Circ Physiol* 2012; **303**: H386–392.
4. Parikh A, Patel D, McTiernan CF, Xiang W, Haney J, Yang L, *et al*. Relaxin suppresses atrial fibrillation by reversing fibrosis and myocyte hypertrophy and increasing conduction velocity and sodium current in spontaneously hypertensive rat hearts. *Circ Res* 2013; **113**: 313–321.
5. Yue L, Feng J, Gaspo R, Li GR, Wang Z, Nattel S. Ionic remodeling underlying action potential changes in a canine model of atrial fibrillation. *Circ Res* 1997; **81**: 512–525.
6. Zhang Y, Wang HM, Wang YZ, Zhang YY, Jin XX, Zhao Y, *et al.* Increment of late sodium currents in the left atrial myocytes and its potential contribution to increased susceptibility of atrial fibrillation in castrated male mice. *Heart Rhythm* 2017; **14**: 1073–1080.
7. Justo F, Fuller H, Nearing BD, Rajamani S, Belardinelli L, Verrier RL. Inhibition of the cardiac late sodium current with eleclazine protects against ischemia-induced vulnerability to atrial fibrillation and reduces atrial and ventricular repolarization abnormalities in the absence and presence of concurrent adrenergic stimulation. *Heart Rhythm* 2016; **13**: 1860–1867.
8. Li Y, Wang S, Liu Y, Li Z, Yang X, Wang H, *et al*. Effect of alpha-allocryptopine on transient outward potassium current in rabbit ventricular myocytes. *Cardiology* 2008; **111**: 229–236.
9. Liu MH, Li Y, Wen Y, Wang L. The effect of allocryptopine on arrhythmia and monophasic action potential in animal models. *Chin J Mult Organ Dis Elder* 2006; **5**: 48–50.
10. Zhang J, Chen Y, Yang J, Xu B, Wen Y, Xiang G, *et al*. Electrophysiological and trafficking defects of the SCN5A T353I mutation in Brugada syndrome are rescued by alpha-allocryptopine. *Eur J Pharmacol* 2015; **746**: 333–343.
11. Kannel WB, Wolf PA, Benjamin EJ, Levy D. Prevalence, incidence, prognosis, and predisposing conditions for atrial fibrillation: population-based estimates. *Am J Cardiol* 1998; **82**: 2N–9N.
12. Aksnes TA, Flaa A, Strand A, Kjeldsen SE. Prevention of new-onset atrial fibrillation and its predictors with angiotensin II-receptor blockers in the treatment of hypertension and heart failure. *J Hypertens* 2007; **25**(1): 15–23.
13. Maltsev VA, Silverman N, Sabbah HN, Undrovinas AI. Chronic heart failure slows late sodium current in human and canine ventricular myocytes: implications for repolarization variability. *Eur J Heart Fail* 2007; **9**: 219–27.
14. Song Y, Shryock JC, Wagner S, Maier LS, Belardinelli L. Blocking late sodium current reduces hydrogen peroxide-induced arrhythmogenic activity and contractile dysfunction. *J Pharmacol Exp Ther* 2006; **318**: 214–222.
15. Chang PC, Huang YC, Lee HL, Chang GJ, Chu Y, Wen MS, *et al.* Inhomogeneous downregulation of INa underlies piceatannol proarrhythmic mechanism in regional ischemia-reperfusion. *Pacing Clin Electrophysiol* **2018; 41**(9): 1116–1122.
16. Dybkova N, Ahmad S, Pabel S, Tirilomis P, Hartmann N, Fischer TH, *et al*. Differential regulation of sodium channels as a novel proarrhythmic mechanism in the human failing heart. *Cardiovasc Res* **2018; 114**(13): 1728–1737.
17. Ahmad S, Tirilomis P, Pabel S, Dybkova N, Hartmann N, Molina CE, *et al.* The functional consequences of sodium channel NaV 1.8 in human left ventricular hypertrophy. *ESC Heart Fail* **2018 Oct 30.** doi: 10.1002/ehf2.12378.
18. Abe K, Machida T, Sumitomo N, Yamamoto H, Ohkubo K, Watanabe I, *et al*. Sodium channelopathy underlying familial sick sinus syndrome with early onset and predominantly male characteristics. *Circ Arrhythm Electrophysiol* **2014; 7**(3): 511–517.
19. Sossalla S, Kallmeyer B, Wagner S, Mazur M, Maurer U, Toischer K, *et al.* Altered Na(+) currents in atrial fibrillation effects of ranolazine on arrhythmias and contractility in human atrial myocardium. *J Am Coll Cardiol* 2010; **55**: 2330–2342.
20. Nattel S, Dobrev D. The multidimensional role of calcium in atrial fibrillation pathophysiology: mechanistic insights and therapeutic opportunities. *Eur Heart J* 2012; **33**: 1870–1877.
21. Blana A, Kaese S, Fortmüller L, Laakmann S, Damke D, van Bragt K, *et al*. Knock-in gain-of-function sodium channel mutation prolongs atrial action potentials and alters atrial vulnerability. *Heart Rhythm* 2010; **7**: 1862–1869.
22. Yu S, Li G, Huang CL, Lei M, Wu L. Late sodium current associated cardiac electrophysiological and mechanical dysfunction. *Pflugers Arch* 2018; **470**(3): 461–469.
23. Burashnikov A. Late INa inhibition as an antiarrhythmic strategy. *J Cardiovasc Pharmacol* 2017; **70**(3): 159–167.

24. Ruan Y, Denegri M, Liu N, Bachetti T, Seregni M, Morotti S, *et al*. Trafficking defects and gating abnormalities of a novel SCN5A mutation question gene-specific therapy in long QT syndrome type 3. *Circ Res* 2010; **106**: 1374–1383.
25. Pezhouman A, Cao H, Fishbein MC, Belardinelli L, Weiss JN, Karagueuzian HS. Atrial fibrillation initiated by early afterdepolarization-mediated triggered activity during acute oxidative stress: efficacy of late sodium current blockade. *J Heart Health* 2018; **4**(1). doi: 10.16966/2379-769X.146.
26. Carneiro JS, Bento AS, Bacic D, Nearing BD, Rajamani S, Belardinelli L, *et al*. The selective cardiac late sodium current inhibitor GS-458967 suppresses autonomically triggered atrial fibrillation in an intact porcine model. *J Cardiovasc Electrophysiol* 2015; **26**(12): 1364–**136**9.
27. Strege P, Beyder A, Bernard C, Crespo-Diaz R, Behfar A, Terzic A, *et al.* Ranolazine inhibits shear sensitivity of endogenous Na^+ current and spontaneous action potentials in HL-1 cells. *Channels* 2012; **6**: 457–462.
28. Pignier C, Rougier JS, Vié B, Culié C, Verscheure Y, Vacher B, *et al*. Selective inhibition of persistent sodium current by F 15845 prevents ischaemia-induced arrhythmias. *Br J Pharmacol* 2010; **161**: 79–91.
29. Xu B, Fu Y, Liu L, Lin K, Zhao X, Zhang Y, *et al*. Effect of α-allocryptopine on delayed afterdepolarizations and triggered activities in mice cardiomyocytes treated with isoproterenol. *Evid Based Complement Alternat Med* **2015; 634172**. doi: 10.1155/2015/634172.
30. Yan J, Zhao W, Thomson JK, Gao X, DeMarco DM, Carrillo E, *et al*. Stress signaling JNK2 crosstalk with CaMKII underlies enhanced atrial arrhythmogenesis. *Circ Res* **2018; 16**; **122**(6): 821–835.
31. Davis RJ. Signal transduction by the JNK group of map kinases. *Cell* 2000; **103**: 239–252
32. Yan J, Thomson JK, Zhao W, Wu X, Gao X, DeMarco D, *et al*. The stress kinase JNK regulates gap junction Cx43 gene expression and promotes atrial fibrillation in the aged heart. *J Mol Cell Cardiol* 2017; **11**4: 105–115.
33. Yan J, Thomson JK, Zhao W, Gao X, Huang F, Chen B, *et al*. Role of stress kinase JNK in binge alcohol-evoked atrial arrhythmia. *J Am Coll Cardiol* 2018; **71**(13): 1459–1470.